https://doi.org/10.54361/ajmas.258382

Original article

Gravitational Lensing as a Window into the Distant Universe: The Complex Interplay of Gravity and Plasma in Lensing Effects

Mohamed Emtir

Technical College of Applied Sciences – Al-Awata, Libya
Email. *mohamedali2013.uk@gmail.com*

Abstract
In this article, we provide a summary of recent advancements concerning the influence of plasma on gravitational lensing effects. The bending of light due to gravity and plasma results from a complex interplay of different physical factors: gravity, dispersion, and refraction. In a non-uniform plasma, chromatic refraction also occurs. We explore chromatic effects in strong gravitational lensing configurations, focusing on the variation in the angular position of the images. Furthermore, we analyse the higher-order images that emerge when lensing occurs around a black hole embedded in a uniform plasma. In this work, we analytically study the time delay for strong gravitational lensing in plasma, including contributions from geometric delay along a bent trajectory in both gravity and plasma, it is conceivable that the ray may be subject to a delay within the gravitational field of the lens, in addition to a dispersion delay that is triggered by the deceleration of light in the medium. In this paper, an expression for the deflection angle is derived in a non-Schwarzschild space-time in the weak field regime in the presence of a plasma. It is demonstrated that this expression depends on the frequency of electromagnetic waves, the gravitational mass M, and the deformation parameter ϵ.
Keywords. Plasma; Gravitational Lensing; Time Delay; Non-Schwarzschild Gravitating Object.

Introduction

The theory of gravitational lensing describes a wide range of phenomena connected with the deflection of light by gravity. These effects include a change in the apparent angular position of the source, multiple imaging, magnification (change in flux), distortion (change in shape) and time delay. Gravitational lensing is currently a powerful astrophysical tool for investigating distant objects, the distribution of dark matter, large-scale structures, the cosmic microwave background, the discovery of planets and the testing of general relativity. In the present paper, we discuss how the presence of plasma may influence the various effects of gravitational lensing. The most straightforward approach to incorporating plasma into the gravitational lensing problem is to consider scenarios where both deflection angles, attributable to gravity and to refraction in the plasma, are negligible. These angles can then be calculated independently from one another. In order to calculate the gravitational angle of deflection, it is sufficient to utilise the linearised theory of gravitation, that is to say, the approximate Einstein formula for the deflection angle. In order to calculate the refraction, it is possible to assume that the refractive index of the plasma differs only slightly from unity (i.e. that it is approximately equal to vacuum) [1].

Since the 1960s, researchers have studied how gravity and refraction interact in the context of the propagation of radio signals in the solar corona. The phenomenon of light deflection, observed when rays of light pass in proximity to the Sun, is attributed to the combined effects of solar gravity and the presence of plasma in the solar corona. In this instance, the deflection resulting from refraction is chromatic in nature, implying that it is contingent on the frequency of the photon.

In strong lens systems with multiple images, the time delay between images is subject to variation, with different images exhibiting distinct delays. The measurement of these delays is a fundamental aspect of the analysis. The observation of the time delay has been proven to be a reliable method for determining the Hubble constant. In the event of the gravitational lens being surrounded by non-homogeneous plasma, chromatic refraction occurs in addition to the vacuum gravitational deflection. Consequently, a variety of chromatic effects may be observed. As outlined in the subsequent section, this is anticipated. Furthermore, it has been established that the speed of signal propagation is reduced relative to the vacuum. This phenomenon is exemplified by the measured time delay of the signal at varying radio frequencies from pulsars in the interstellar medium [2,3].

The non-Schwarzschild spacetime has been introduced, wherein two large classes of alternative theories were studied, modifying the action through algebraic, quadratic curvature invariants coupled to scalar fields. The investigation of astrophysical phenomena in the vicinity of deformed compact gravitational objects could provide a valuable opportunity for constraining the allowed parameter space of solutions. In addition to providing a deeper insight into the physical nature and properties of the corresponding spacetime metric, such studies could also yield novel scientific insights [4]. A part of the principal aim of this study is to investigate the weak gravitational lensing of a non-Schwarzschild compact object by a homogeneous plasma, and to determine the effect of the plasma's deformation parameter on the deflection angle in the weak field regime.

Received*: 21-06-2025 -* ***Accepted****: 19-08-2025 -* ***Published****: 26-08-2025*

Methods

Refraction in Inhomogeneous Media: Light has Curved Trajectories in Space

The theory of gravitational lensing accounts for a variety of effects associated with light being deflected by gravity: apparent angular position shift, multiple imaging, flux magnification (change in the amount of the flux), shape distortion (change of the form), and time delay.

Strong Gravitational Lensing: Implications of Weak Deflection Approximation

The most spectacular manifestation of gravitational lensing is multiple images of the same source; we will demonstrate how it works for the simplest case of a point-mass lens. For a strong lens system, the distribution of matter in the lens is more complex than a point mass and must have essential deviations from spherical symmetry (or any other kind of symmetry), but each small patch of matter still deflects light according to the approximate Einstein formula.

Gravitational Lensing Effects: Primary and High-Order Image Schemes

As the photons approach the black hole, photons with impact parameters greater than a critical value are predicted to return to infinity, thus confirming the theoretical predictions of general relativity.

Einstein Rings and Relativistic Rings: Explained Through Gravitational Lensing

The strong deflection limit ensures a high degree of accuracy for photons that have undergone one or more turns, thus facilitating the calculation of the properties of relativistic images and Einstein rings. In particular, it has been demonstrated that for any spherically symmetrical space-time, the deflection angle exhibits a logarithmic divergence as the impact parameter approaches its critical value.

The Interplay of Gravity and Plasma in Weak Deflection Scenarios in the Schwarzschild Metric

In the following section, an attempt is made to calculate the photon deflection angle in circumstances involving both gravitation and plasma.

Weak Deflection in Homogeneous Plasma: Analytical Approach

For a homogeneous plasma where ω_{ep}^2 is a constant, the refractive index is found to be space coordinate-independent, resulting in the absence of refractive action. Therefore, in the case of homogeneity, the angle $\hat{\alpha}_{def}$ may be considered as the gravitational deflection in a given medium (plasma). Notwithstanding the absence of deflection resulting from refraction, this deflection deviates from vacuum gravitational deflection.

Weak Deflection in Non-Homogeneous Plasma: Analytical Approach

In the event of plasma non-homogeneity, the refractive deflection α_{refr}, must also be considered. The methodology for gravitational lensing in plasma, as developed in [1, 2], facilitates the concurrent consideration of two effects:

(i) The gravitational deflection observed in a plasma deviate from the theoretical Einstein angle.

(ii) Refraction is observed to be connected with plasma inhomogeneity, a phenomenon which is independent of gravity.

The Interplay of Gravity and Plasma in Strong Lens Scenarios

Chromatic gravitational lensing is invariably caused by the presence of plasma. In a plasma where all the particles have the same properties, the colour effects are caused by the different gravitational deflection. An additional chromatic refractive deflection occurs in the case of a non-homogeneous plasma.

Plasma's Role in Shifts of Angular Position in Lensing

For a strong lens system, the weak deflection approximation is sufficient. For a homogeneous plasma and a point-mass lens, formula (7) can be used. If it is also assumed that the plasma frequency is much smaller than the photon frequency, formula (8) can be used. Formula (14) is all that's needed for a non-homogeneous plasma and a point-mass lens.

Time Delay Analysis in Simultaneous presence of Gravity-Plasma Scenarios: analytical approach

An investigation into the time delay in the case of gravitational lensing in plasma is conducted, with a particular focus on strong lens systems. It is approached analytically, leading to the identification of compact expressions for plasma corrections, which are instrumental in the estimation process. The terms 'strong lens system' and 'strong lensing' are employed to denote an observational situation in which a gravitational lens produces multiple images.

Plasma's Influence on Black Hole Lensing: A Detailed Analysis

The Schwarzschild black hole is considered, with a discussion of the influence of plasma on the positions and magnifications of high-order (relativistic) images. The calculation of the angle of deflection of a weak photon can be achieved through the use of Einstein's formula.

Received*: 21-06-2025 -* ***Accepted****: 19-08-2025 -* ***Published****: 26-08-2025*

The Interplay of Plasma and Non-Schwarzschild Lensing Effects: Angle of Deflection in Asymptotic Flatness

The principal aim of this section is also to undertake a detailed investigation into the weak gravitational lensing of a compact object by a non-Schwarzschild nature, in the presence of a homogeneous plasma. The investigation will ascertain the impact of the plasma on the deformation parameter and its subsequent effect on the deflection angle, within the weak field limit.

Results and Discussion

Refraction in Inhomogeneous Media: Light has Curved Trajectories in Space

In outer space, the propagation of light rays through plasma has been observed. In plasma, photons are subject to a variety of effects, including absorption, scattering and refraction. In the context of gravitational lensing, which is typically employed within the framework of geometric optics, the primary focus lies in the modification of the angle of deflection of a light ray. It is reasonable to hypothesise that chromatic effects will also arise due to the dispersion properties of plasma.

It is widely acknowledged that light rays propagate along curved trajectories in a transparent and inhomogeneous medium [3,4]. This phenomenon is known as refraction and is a well-known occurrence in everyday life. As a case in point, the refractive effect causes the image to deviate from its true form when observed through the optical lens. A spoon appears to be fractured when placed in a glass of water, and the depth of the pond appears to be less than it actually is in reality. It is evident from (Figure 1) that the bending of light rays due to refraction is unrelated to relativity or gravity and occurs only if the medium is optically non-homogeneous.

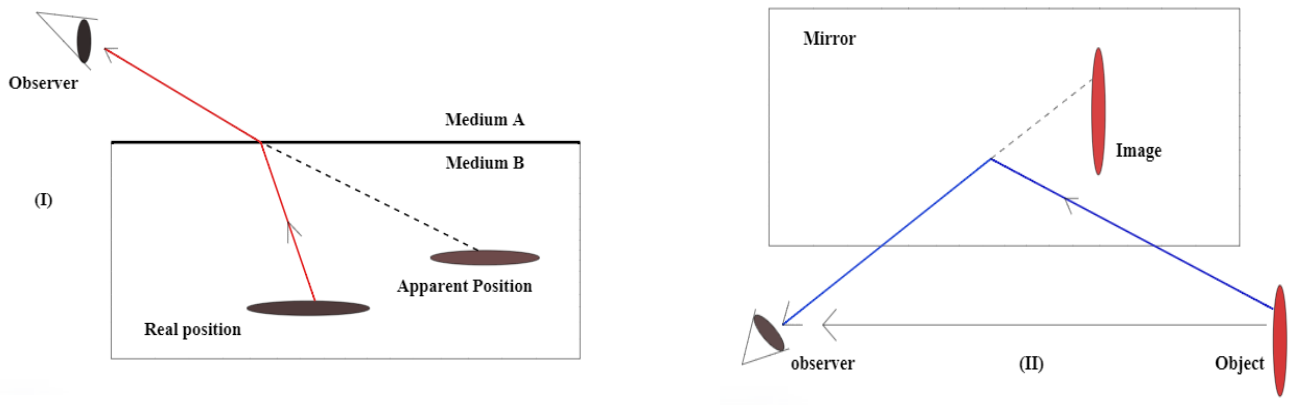

Figure 1. Exhibits effects analogous to those of gravitational lensing, yet these effects are attributed to the non-homogeneity of the medium.

Strong Gravitational Lensing: Implications of Weak Deflection Approximation

At the current level of observational development, chromatic effects resulting from lensing in a plasma may only be observed in a strong lens system. It is anticipated that the observation of images in different wavelengths will yield distinct angular positions, a phenomenon attributable to the presence of plasma. By measuring the difference in angular positions, we can obtain information about the distribution of the plasma in the lens. As illustrated in (Figure 2), the image on the left provides a visual representation of the positions of the images observed from the observer's perspective. The Einstein ring is denoted by a dashed circle.

Received*: 21-06-2025 -* ***Accepted****: 19-08-2025 -* ***Published****: 26-08-2025*

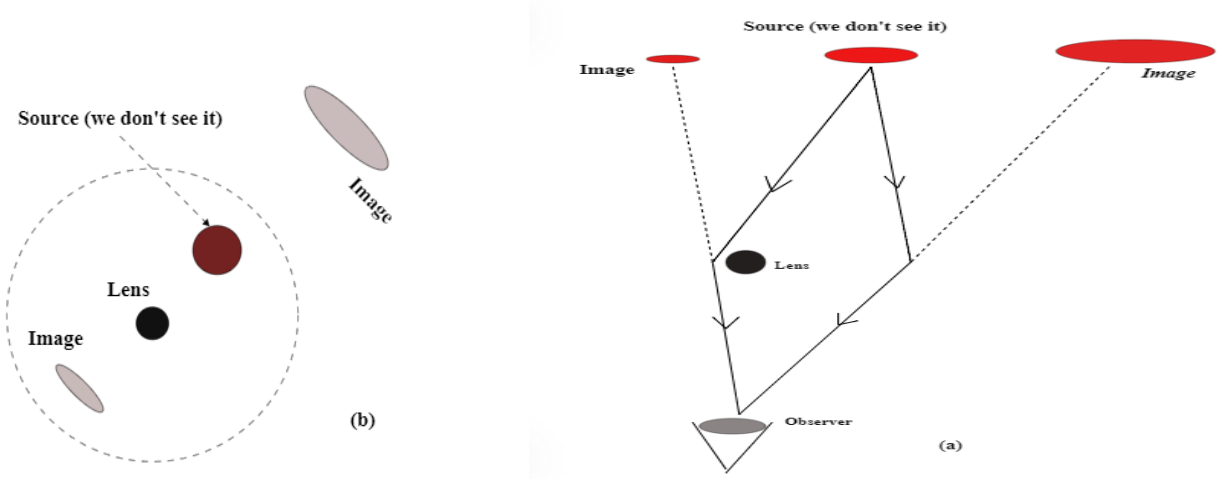

Figure 2. Gravitational lensing in a vacuum can result in the formation of multiple images of the source.

Gravitational Lensing Effects: Primary and High-Order Image Schemes

In gravitational lensing on a black hole, two distinct images of the source are initially formed. The first and the second images are ordinary and are formed by photons with a frequency greater than 2π. In addition to these images, two infinite sequences of high-order images are formed. They are formed by photons with a frequency greater than 2π. The Schwarzschild metric is what determines the trajectory of light rays. The light ray from the source is deflected by the point-mass gravitational lens and subsequently arrives at the observer. The image perceived by the observer is positioned at an angular distance, designated as θ, from the actual source position. The concept of R is defined as the closest point of the trajectory to the gravitating centre. This point is commonly referred to as the distance of closest approach. The parameter b is known as the impact parameter of the photon (see Figure 3).

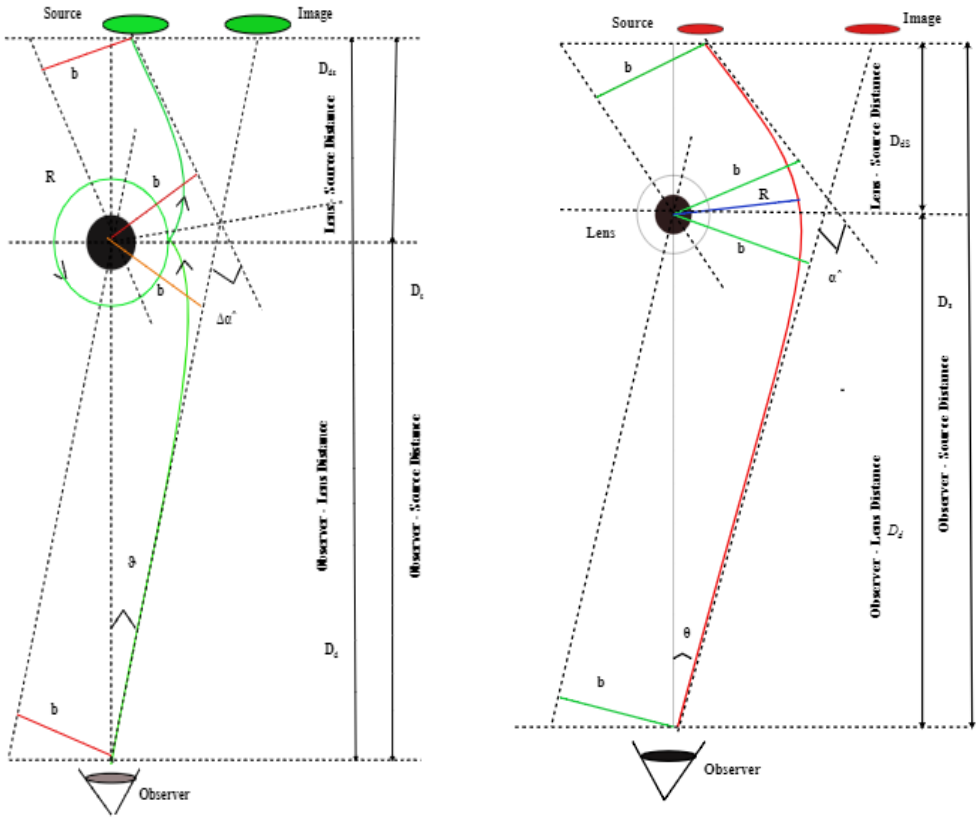

Figure 3. Illustrates the formation of primary (right) and high-order (lift) images of the source in the context of gravitational lensing by a black hole in a vacuum.

Einstein Rings and Relativistic Rings: Explained Through Gravitational Lensing

It is evident that the calculation of relativistic images can be achieved by employing the exact deflection angle in the lens equation. It has been demonstrated that this function possesses a form of the integral, and

Received: *21-06-2025* - ***Accepted***: *19-08-2025* - ***Published***: *26-08-2025*

can be expressed via an elliptic integral [5,6]. The investigation of relativistic images is facilitated by the utilisation of the so-called strong deflection approximation, which is the antithesis of the weak deflection approximation. Relativistic rings (see Figure 4) were the subject of detailed investigation in work [6]. As the impact parameter approaches the critical value, the deflection angle logarithmically diverges. As indicated in the work of Darwin [5,7]. The logarithmically divergent expression for the photon deflection angle in a vacuum in the strong deflection limit was obtained for the Schwarzschild metric.

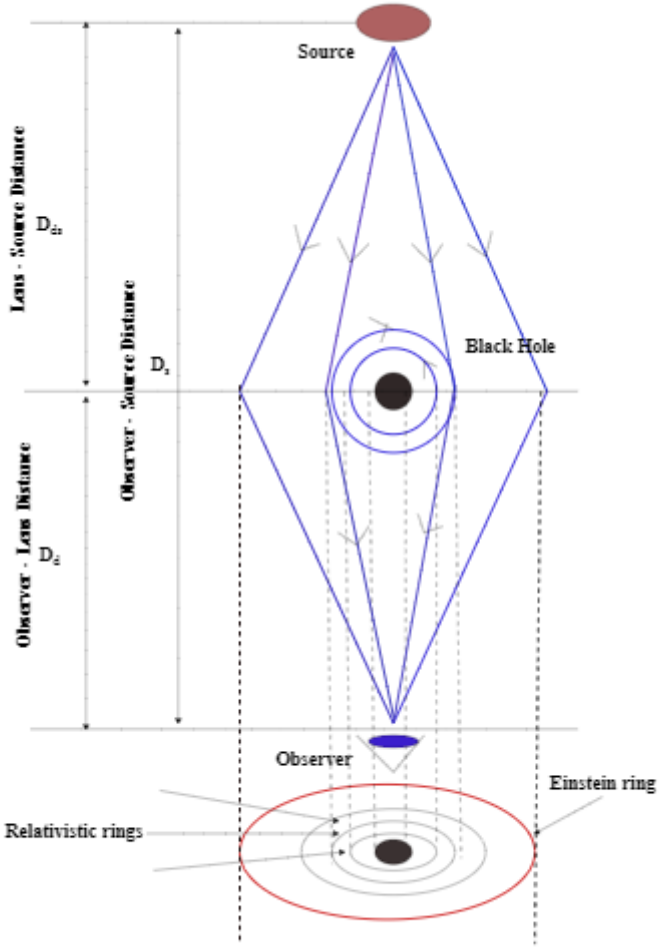

Figure 4. The phenomenon of Einstein rings, as well as relativistic rings, is attributable to the occurrence of black hole lensing.

The Interplay of Gravity and Plasma in Weak Deflection Scenarios in the Schwarzschild Metric

The following hypothesis is put forward for consideration: What would happen if the closest approach distance were much larger than the Schwarzschild radius? It means:

$$R \gg M (R_s = 2M)$$

Weak Deflection in Homogeneous Plasma: Analytical Approach

It is also important to note that, during the motion, the r-coordinate changes from R to infinity, i.e. $r \gg M$, and the resulting deflection angle is small, i.e. $\hat{\alpha}_{def} \ll 1$. The deflection angle can be expressed as follows:

$$\hat{\alpha}_{def} = -\pi + 2\int_R^{\infty} \left(r\sqrt{1-\frac{2M}{r}}\right)^{-1} \left(\sqrt{\frac{h^2(r)}{h^2(R)}-1}\right)^{-1} dr \quad (1)$$

$$h(r) = r\left(\frac{1}{1-2M/r} - \frac{\omega_{ep}^2}{\omega^2}\right)^{1/2} \quad (2)$$

Considering the case with ω_{ep}^2= const. We denote $\omega_{ep}^2/\ \omega^2 = F$, using that $R \gg M$ and r $\gg M$. substituting for $h(r)$ and $h(R)$ in eq. 2 into eq. 1. We obtain

$$\frac{h^2(r)}{h^2(R)} \cong R\left[\frac{M}{1-F}\ \frac{(r-R)r}{(r^2-R^2)R} + 1\right](r^2-R^2)^{-1/2} \quad (3)$$

Received: *21-06-2025* - ***Accepted***: *19-08-2025* - ***Published***: *26-08-2025*

and

$$\frac{1}{r}\left(1-\frac{2M}{r}\right)^{-1/2} \cong \frac{1}{r}\left(1+\frac{M}{r}\right) \quad (4)$$

We get

$$\hat{\alpha_{def}} = 2MR^{-1}\left(\frac{1}{1-F}+1\right) \quad (5)$$

Or, in ordinary units,

$$\hat{\alpha_{def}} = \frac{R_S}{R}\left(\frac{1}{1-F}+1\right), \qquad R_s = \frac{2GM}{c^2}, \quad F = {\omega_{ep}}^2/{\omega_0}^2 \quad (6)$$

We need to know how angles depend on the impact parameter, b. In the approximation $R \gg M$, the difference between R and b is negligible, so we can substitute $R \cong b$ into (5) to obtain:

$$\hat{\alpha_{def}} = \frac{2M}{b}\left(\frac{1}{1-F}+1\right) \quad (7)$$

It is evident that formula (7) is only applicable when $\omega_0 > \omega_{ep}$, due to the fact that waves with $\omega_0 < \omega_{ep}$ do not propagate within a plasma. As the gravitational deflection in plasma is known to be significantly larger than in a vacuum, it is imperative to consider the conditions for this to occur.

$$\hat{\alpha_{def}} = \alpha_{vacu} + \alpha_{corr} = \frac{2R_S}{b}\left(1+\frac{\omega_{ep}^2}{2{\omega_0}^2}\right) \quad (8)$$

$\left(\alpha_{vacu} = \frac{2R_s}{b}\right)$, is the vacuum gravitational deflection and $\left(\alpha_{corr} = \frac{R_S}{b}\frac{\omega_{ep}^2}{{\omega_0}^2}\right)$, is an additional correction to the gravitational deflection connected with the plasma presence.

Weak Deflection in Non-Homogeneous Plasma: Analytical approach

Expanding the exact integral Formula (8) with $M/r \ll 1$ and $\omega_{ep}^2(r)/\omega_0^2 \ll 1$We obtain an approximate formula for the case of a weak deflection in a non-homogeneous plasma

$$\alpha_{Refr} = R\int_R^\infty (r^2-R^2)^{-1/2}\frac{dF}{dr}dr, \quad F = \omega_{ep}^2/\omega_0^2 \quad (9)$$

$$= \frac{RK_{ep}}{\omega^2}\int_R^\infty (r^2-R^2)^{-1/2}\frac{dN(r)}{dr}dr, \quad K_{ep} \equiv \frac{4\pi}{m}e^2 \quad (10)$$

For gravitational lensing, the dependence of angles on the impact parameter b is needed. In papers [1,2], we have derived $\hat{\alpha}_{Ref}$ using Cartesian coordinates. We have considered the photon with the unperturbed trajectory as a straight line parallel to the z-axis, with the impact parameter $b \cong R \gg M$. In this case, we have, at a given b:

$$\frac{\partial N}{\partial b} = \frac{dN}{dr}\frac{\partial r}{\partial b} = \frac{dN}{Dr}\frac{b}{r} \quad (11)$$

Integral with respect to $r \quad \rightarrow \quad$ integral with respect to z, at b const.

$$dr = d(b^2-z^2)^{1/2} = \frac{z}{r}dz \quad (12)$$

Changing $R \rightarrow b$, $(R = b)$

$$z = (r^2-R^2)^{1/2}, \quad \frac{dN}{dr} = \frac{r}{b}\frac{\partial N}{\partial b}, \quad dr = \frac{z}{r}dz \quad (13)$$

$$\alpha_{refr} = \frac{bK_{ep}}{\omega_0^2}\int_0^\infty \frac{1}{z}\frac{r}{b}\frac{\partial N}{\partial b}\frac{z}{r}\,dz = \frac{K_{ep}}{\omega_0^2}\int_0^\infty \frac{\partial N}{\partial b}\,dz \quad (14)$$

We have,

$$\hat{\alpha}_{Ref} = \alpha_{Vacu} + \alpha_{refr} \quad (15)$$

$$\hat{\alpha}_{Ref} = \frac{2R_s}{b} + \frac{K_{ep}}{\omega_0^2}\int_0^\infty \frac{\partial N}{\partial b}\,dz \quad (16)$$

The presence of homogeneous or non-homogeneous plasma has been demonstrated to increase the gravitational deflection of photons. It is generally accepted that a vacuum gravitational deflection is positive ($\alpha_{Vacu} > 0$). Consequently, the additional correction to gravitational deflection resulting from the presence of plasma is also positive ($\alpha_{corr} > 0$). It is evident that the density of plasma typically decreases with radius across different models ($dN/dr < 0$). Consequently, the refractive deflection is generally opposite to the gravitational deflection. The correction due to refractive deflection is negative ($\alpha_{Refr} < 0$), as can be seen in [2].

Received: *21-06-2025* - ***Accepted***: *19-08-2025* - ***Published***: *26-08-2025*

The Interplay of Gravity and Plasma in Strong Lens Scenarios

The observational effects of frequency dependence can be explained by referring to the Schwarzschild point-mass lens [1,2]. In order to ascertain the discrepancy in the angular position of images, a comparison of radio and optical observations of images is required.

Plasma's Role in Shifts of Angular Position in Lensing

When it comes to optical frequencies, the impact of plasma is found to be negligible. Consequently, the calculation of image positions can be performed utilising vacuum formulae (See figure 5).

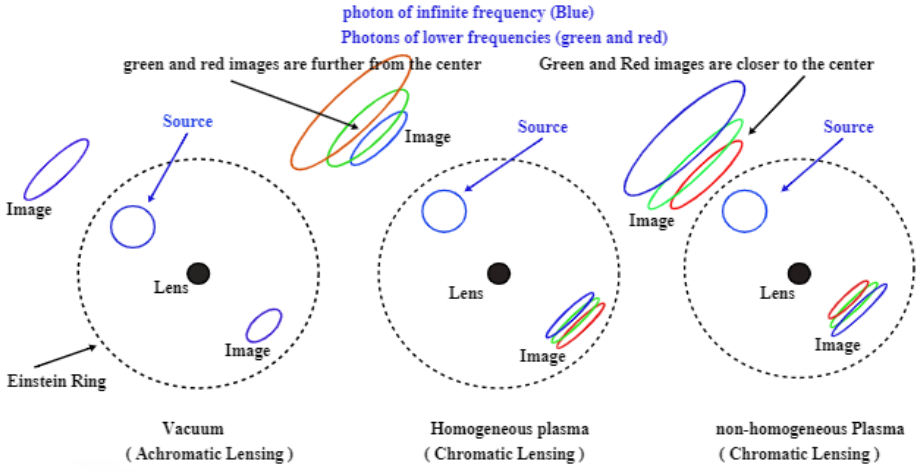

Figure 5. Shows a schematic comparison of lensing by point mass in plasma (middle and right) and in vacuum (left)

With regard to the theory of refractive plasma deflection, the authors have taken into consideration two models of plasma. The initial object under consideration is a spiral galaxy characterised by a high concentration of plasma.

$$N(r) = N_0 e^{-r/r_0} \tag{17}$$

The radius r is measured from the centre of the galaxy. The constants are $N_0 = 10\text{cm}^{-3}$ and $r_0 = 10\text{kpc}$. The second plasma model is used for elliptical galaxies:

$$N(r) = N_0 \left(\frac{r}{r_0}\right)^{-1.25} \tag{18}$$

with $N_0 = 0.1\ \text{cm}^{-3}$ and $r_0 = 10\text{kpc}$. These values of N_0 correspond to the plasma frequency we $\omega_{ep} \cong 1.8 \times 10^5\ \text{sec}^{-1}$ and $1.8 \times 10^4\ \text{sec}^{-1}$.

Time Delay Analysis in Simultaneous Presence of Gravity-Plasma.

In this section, the time delay in the presence of both a gravitational lens and plasma will be considered. The total deflection of a light ray is expressed as the aggregate of two constituent components: namely, vacuum gravitational deflection and refractive plasma deflection.

$$\hat{\alpha}_{def} = \hat{\alpha}_{gra} + \hat{\alpha}_{ref}\ ; \quad \hat{\alpha}_{gra}, \hat{\alpha}_{ref} \ll 1 \tag{19}$$

It is hypothesised that both angles are negligible and independent of each other. The effects of gravity and plasma are considered in linear order; all other mixed and higher-order terms are neglected in this instance. In accordance with the aforementioned approximations, the following contributions to time delay are considered, in comparison with straight-line propagation in a vacuum in the absence of gravity:
(i) the geometric delay Δt^{GEOM} associated with additional path length due to the bending of the trajectory in the presence of both gravity and plasma;
(ii) the potential delay Δt^{POT} of the ray caused by the time retardation of the ray while moving in the gravitational field of the lens;
(iii) the dispersion delay Δt^{DISP} in the plasma associated with a decrease in the signal velocity in the medium.

Received: *21-06-2025* - ***Accepted***: *19-08-2025* - ***Published***: *26-08-2025*

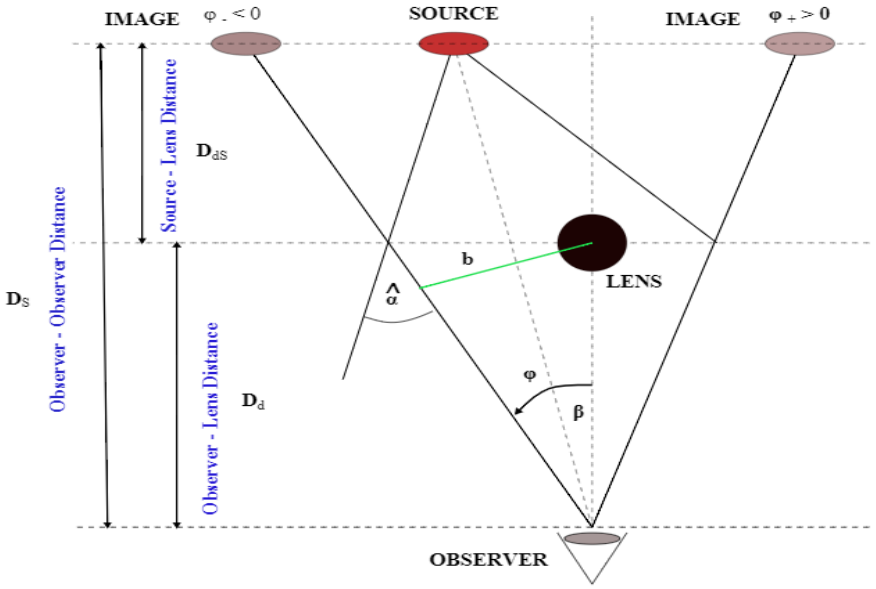

Figure 6. The standard pattern of gravitational lensing: The way light travels from a distant source at an angle (β), as seen by the observer. The lens deflects the light at an angle (α̂), creating an observation angle (φ).

The assumption is made that both the lens and the surrounding plasma exhibit spherical symmetry. Consequently, one-dimensional variables can be employed in the lens equation and the time delay expressions. It should be noted that, in the general case, the positions of the source and images are described by two-dimensional quantities in the source plane and lens plane, respectively. Nevertheless, in the case of axially symmetric scenarios, it is feasible to transition to one-dimensional values in the lens equation. This will subsequently be delineated in the plane where all rays forming images are situated (see Figure 6). The geometrical delay [8, 9] is defined as follows:

$$\Delta t^{GEOM}(\varphi) = \frac{z_d+1}{c}\frac{D_d D_s}{D_{ds}}\frac{(\varphi-\beta)^2}{2} \qquad (20)$$

where β is the angular position of the source, whereas φ is the position of the image. Additionally, z_d denotes the redshift of the lens, and D_j represent angular diameter distances, as illustrated in (Figure 6). The form of expression (20) is universally applicable, in the sense that it can be used for deflection caused by any physical reason. Its utilisation extends beyond the domain of vacuum gravitational lensing, encompassing applications in plasma lensing as well [10,11]. The significance of geometric delay in comparison with potential delay was addressed in [12.13]. Similarly, the potential delay [14-16]:

$$\Delta t^{POT}(\varphi) = \frac{z_d+1}{c}\frac{D_d D_s}{D_{ds}}\psi(\varphi) + C \qquad (21)$$

$\psi(\varphi)$, is to be understood as the deflection potential [17-19], the definition of which is such that the gradient of this potential is equal to the deflection angle. The potential is dependent upon the mass distribution in the lens.

$$\alpha = \Delta\psi, \quad \alpha = \frac{D_{ds}}{D_s}\hat{\alpha}_{def} \qquad (22)$$

In this investigation, the dispersive delay is analysed in cold, non-magnetised plasma with a refractive index of n:

$$n = \sqrt{1-\frac{\omega_{ep}^2}{\omega^2}}, \qquad \omega_{ep}^2 = \frac{4\pi e^2}{m_e}N_e \qquad (23)$$

In this equation, ω_{ep}^2 denotes the plasma electron frequency, ω signifies the photon frequency (as measured locally), m_e and e represent the electron mass and charge, respectively, and N_e designates the electron number density in the plasma. In the linearised approximation, with gravitational and plasma terms treated

Received: *21-06-2025* - ***Accepted***: *19-08-2025* - ***Published***: *26-08-2025*

separately, the change in the frequency of photons due to the gravitational field (i.e. gravitational redshift) can be neglected in terms containing plasma. It is imperative to note that this cannot be neglected if greater precision is required in the calculation of plasma effects, for instance, when determining corrections to the vacuum gravitational deflection due to the presence of a homogeneous plasma [20,21], or in the case of black hole shadow determination [22-24].

$$n^2 \approx 1 - \frac{\omega_{ep}^2}{2\omega^2} = 1 - \frac{2\pi e^2}{m_e \omega^2} N_e \tag{24}$$

and for the delay of a ray in a plasma compared to its propagation in a vacuum, we write:

$$\Delta t = \frac{1}{c}\int \left(\frac{1}{n} - 1\right) dl = \frac{2\pi e^2}{m_e \omega^2 c} N_{inten}\,, \quad N_{inten} = \int N_e dl \tag{25}$$

In this particular instance, N_{inten} denotes the projected electron density along the line of sight, which is more commonly referred to as the dispersion measure (DM). When combined with the cosmological factor, the following equation is obtained:

$$\Delta t^{disp} = \frac{z_d+1}{c}\frac{2\pi e^2}{m_e \omega^2 c} N_{int} \tag{26}$$

as a result, the formula for the time delay becomes [16]:

$$\Delta t(\varphi) = \left[\frac{(\varphi-\beta)^2}{2} - \psi(\varphi)\right]\frac{DM}{c} + \frac{z_d+1}{c}\frac{K_{ep}}{2\omega^2} N_{int}([\varphi]), K_{ep} = 4\pi e^2/m_e \tag{27}$$

the variable

$$DM = (z_d + 1)\frac{D_d D_s}{D_{ds}} \tag{28}$$

is known as the time-delay distance [18,19].
It is important to note that formula (27) is general; any distribution of gravitating mass in the lens can be considered, thereby defining the function $\psi(\varphi)$in conjunction with the deflection angle, according to equation (22).Moreover, any spherically symmetric distribution of surrounding plasma, given by N_e and $N_{inten}([\varphi])$, can be utilised. It is also observed that the dispersive term manifests itself in both homogeneous and non-homogeneous plasmas.

Plasma's Influence on Black Hole Lensing: A Detailed Analysis

In Darwin's paper [5], it was demonstrated that an additional limiting situation for photons, characterised by multiple circumambulations around a central object, can be examined analytically. In this limit, known as the strong deflection limit, the deflection angle is expressed as [5,7].

$$\begin{aligned}\hat{\alpha}_{def} &= 2\ln\left[12\left(2-\sqrt{3}\right)\right] - 2\ln\left(\frac{R}{r_M} - 1\right) + - \pi \\ &= -2\ln\frac{R-3M}{36\left(2-\sqrt{3}\right)M} - \pi = -2\ln\frac{(2+\sqrt{3})(R-3M)}{36M} - \pi\end{aligned} \tag{29}$$

or, as a function of the impact parameter b [61,62]

$$\begin{aligned}\hat{\alpha}_{def} &= -\ln\left(\frac{b}{b_{cr}} - 1\right) + \ln\left[216\left(7-4\sqrt{3}\right)\right] - \pi \\ &= -\ln\frac{b-3\sqrt{3}M}{648\sqrt{3}(7-4\sqrt{3})M} - \pi = -ln\frac{(7+4\sqrt{3})(b-3\sqrt{3}M)}{648\sqrt{3}M} - \pi\end{aligned} \tag{30}$$

The following discussion will address the impact of plasma presence on relativistic images. In a homogeneous plasma, the photon deflection angle, defined as the angle of deviation of a photon's trajectory from a linear path, is expressed as a function of the closest approach distance, R, and the ratio of frequencies, ω_{ep}^2/ω_0^2, as outlined in reference [25].

$$\hat{\alpha}(R,x) = -2\sqrt{\frac{1}{2}\left(\frac{x+1}{x}\right)}\, ln\left[z_1(x)\frac{R-r_M}{r_M}\right] - \pi \tag{31}$$

where

$$z_1(x) = \frac{9x-1+2\sqrt{6x(3x-1)}}{48x}\,, \quad r_M = \frac{1+x}{1+3x}(6M)\,, \quad x = \left(1 - \frac{8}{9}\omega_{ep}^2/\omega_0^2\right)^{1/2} \tag{32}$$

The formula (31) is asymptotically exact and valid for R close to r_M. It is imperative to acknowledge the significance of the critical (minimum) value of R, which is equivalent to r_M. r_M is defined as the radius of the point at which the maximum of the effective potential is attained. It is evident that the deflection angle of a

Received*: 21-06-2025 -* ***Accepted****: 19-08-2025 -* ***Published****: 26-08-2025*

photon approaches infinity as the radius R approaches r_M. As a consequence, the photon undergoes an infinite number of rotations at the radius r_M.In the event that the condition $\omega_0 \gg \omega_{ep}$ is met, it can be deduced that $x \to 1$, thus resulting $r_M = 3M$. This is analogous to the photon in the vacuum. The deflection angle is defined as a function of the impact parameter b and the ratio of frequencies, expressed as: ω_{ep}^2/ω_0^2.

$$\hat{\alpha}(b,x) = -\sqrt{\frac{1}{2}\left(\frac{x+1}{x}\right)}\ln\left[\frac{b-b_{cr}}{b_{cr}}\frac{2z_1^2(x)}{3x}\right] - \pi, \ \ where \ \ b_{cr} = \sqrt{3}\, r_M \left(\frac{1+x}{3x-1}\right)^{1/2} \tag{33}$$

This formula is valid for b close to b_{cr}, where b_{cr} is a critical value of the impact parameter under the given ω_{ep}^2/ω_0^2. For we $\omega_0 \gg \omega_{ep}$ we obtain the critical impact parameter for vacuum, $b_{cr} = 3\sqrt{3}M$. For simplicity, let us rewrite Formula (33) as

$$\hat{\alpha}(b,x) = -a(x)ln\left(\frac{b-b_{cr}}{b_{cr}}\right) + c(x) \tag{34}$$

where $a(x)$ and $c(x)$ are defined as

$$a(x) = \sqrt{\frac{1}{2}\left(\frac{x+1}{x}\right)}\,, \quad c(x) = -\sqrt{\frac{1}{2}\left(\frac{x+1}{x}\right)}\ln\left(\frac{2}{3}\,\frac{z_1^2(x)}{x}\right) - \pi \tag{35}$$

solving the equation

$$\hat{\alpha}(b,x) = 2\pi k\,, \quad k = 1,2,\dots\,,$$

For a relativistic imaging, the impact parameters $b_k(x)$ and the angular positions of the relativistic images $\vartheta_k(x)$ can be expressed as follows:

$$b_k(x) = b_{cr} = \left[1 + exp\left(\frac{c(x)-2\pi k}{a(x)}\right)\right], \ \ \vartheta_k(x) = \frac{b_{cr}}{D_d}\left[1 + exp\left(\frac{c(x)-2\pi k}{a(x)}\right)\right] \tag{36}$$

The distance between the observer and the lens, D_d, shall be considered. It is evident that the angular positions ϑ_k in plasma invariably exceed those in a vacuum. It can thus be concluded that the presence of homogeneous plasma leads to an increase in the angular separation of point relativistic images from the gravitating centre, or the angular size of the relativistic rings. The magnification of the relativistic images of a point source μ_k situated at an angular position b from the line connecting the observer and the gravitational centre (lens) has been determined to be equal to [25].

$$\mu_k = \frac{D_s b_{cr}^2(1+l_k)}{D_{ds}D_d^2\, a(x)\beta}\,, \quad l_k = exp\left(\frac{c(x)-2\pi k}{a(x)}\right) \tag{37}$$

It is evident that both $a(x)$ and $c(x)$ These are coefficients that have been defined in equation (34). In the expression (37), it can be observed that the variables b_{cr},l_k, $a(x)$, $c(x)$ are contingent on x, thereby indicating a relationship between these variables and the ratio of the photon and the plasma frequencies. It has been established that the magnification μ_k of the relativistic images tends to infinity if the source angular position $b \to 0$, as is the case in the vacuum [26]. As ω_0 approachesω_{ep}It is evident that μ_k experiences an unbounded increase. This phenomenon can be attributed to the fact that b_k approaches infinity in this limit, as demonstrated in Equations (32) and (33) and illustrated in (see Figure 7).
Although the presence of the plasma can significantly increase the magnification compared to the plasma-free case, the magnifications remain very small because the vacuum values are very small. For example, for $M/D_d = 2.26467 \times 10^{-11}$, which corresponds to the supermassive black hole at the centre of the Milky Way $D_s/D_{ds} = 2,\ \beta = 1\,\mu as$These parameters have been taken from [27], the vacuum values of magnification are [25].

$\mu_1^{Vacu} = 0.716 \times 10^{-11},\ \mu_2^{Vacu} = 0.134 \times 10^{-13}\,,\quad \mu_3^{Vacu} = 0.249 \times 10^{-16}$

Received*: 21-06-2025 -* ***Accepted****: 19-08-2025 -* ***Published****: 26-08-2025*

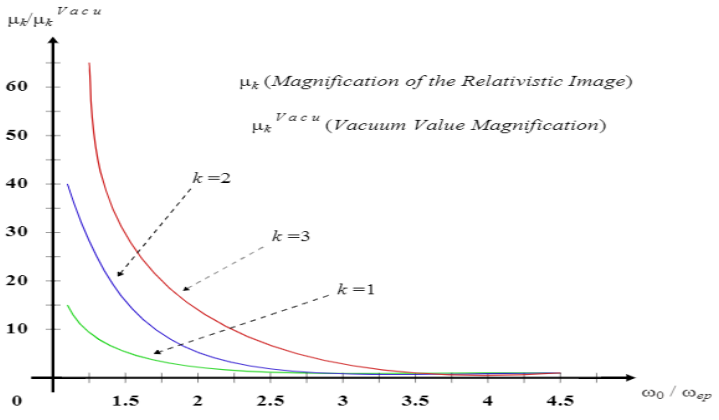

Figure 7. A comparison of the magnification factors of relativistic images for lensing in homogeneous plasma and in vacuum is presented.

The Interplay of Plasma and Non-Schwarzschild Lensing Effects: Angle of Deflection in Asymptotic Flatness

The deformed Schwarzschild-like metric, which describes a static, asymptotically flat, vacuum spacetime in standard Boyer–Lindquist coordinates, can be expressed as follows [1].

$$ds^2 = -\left(1-\frac{2GM}{c^2r}\right)(1+h)c^2dt^2 + f^{-1}(1+h)dr^2 + r^2(d\theta^2 + sin^2\theta d\phi^2) \quad (38)$$

The spacetime metric is understood to comprise parameters that quantify potential discrepancies from the Schwarzschild metric, in conjunction with the lensing object. When $h(r) = 0$, the metric reduces to the Schwarzschild metric in Boyer-Lindquist coordinates. The function $h(r)$ can be selected as:

$$h(r) = \sum_{k=0}^{\infty} \epsilon_k \left(\frac{GM}{c^2r}\right)^k \quad (39)$$

The constraints on $\epsilon = 0$ can be derived from the asymptotic properties of metric (38). The condition for the metric to be asymptotically flat implies that $\epsilon_0 = \epsilon_1 = 0$. Here, we have chosen the function $h(r)$ to be the third power of $2GM/(c^2r)$, as in [2].

$$h(r) = \epsilon\left(\frac{GM}{c^2r}\right)^3 \quad (40)$$

As ϵ approaches zero, the metric (38) reduces to the standard Schwarzschild metric, which is well known in the context of general relativity. In the limit of large radii, the non-Schwarzschild metric of a static and asymptotically flat spacetime can be written as [28]:

$$ds^2 = ds_0^2 + \left(\frac{2GM}{c^2r} - h\right)c^2dt^2 + \left(\frac{2GM}{c^2r} + h\right)dr^2 \quad (41)$$

the flat part of the above metric is as follows:

$$ds_0^2 = -c^2dt^2 + dr^2 + r^2(d\theta^2 + sin^2\theta d\phi^2) \quad (42)$$

In the Cartesian coordinates, the components $h_{\alpha\beta}$ are written as

$$h_{00} = -\left(-\frac{r_g}{r} + h\right) \quad (43)$$

$h_{ik} = \left(\frac{r_g}{r} + h\right)n_i n_k$. $\quad h_{33} = \left(\frac{r_g}{r} + h\right)cos^2\chi, \quad r_g = 2GM/c^2, \quad n_3 = cos\chi = \frac{z}{r} = z/\sqrt{b^2+z^2}$.

The following formula will serve to calculate the deflection angle of light for non-Schwarzschild lensing objects in
a homogeneous plasma:

$$\hat{\alpha}_b = \int_0^{\infty} \frac{\partial}{\partial b}\left[\frac{z^2}{b^2+z^2}\left(\varepsilon\frac{\left(\frac{GM}{c^2}\right)^3}{(b^2+z^2)^{\frac{3}{2}}} + \frac{r_g}{(b^2+z^2)^{1/2}}\right) - \left(\varepsilon\frac{\left(\frac{GM}{c^2}\right)^3}{(b^2+z^2)^{\frac{3}{2}}} - \frac{r_g}{(b^2+z^2)^{1/2}}\right)\frac{1}{1-\frac{\omega_0^2}{\omega^2}}\right]dz \quad (44)$$

the deflection angle as be calculated as

Received: *21-06-2025* - ***Accepted***: *19-08-2025* - ***Published***: *26-08-2025*

$$\hat{\alpha}_b = -\frac{r_g}{b}\left[\varepsilon\left(\frac{GM}{c^2 b}\right)^2\left(\frac{1}{1-\frac{\omega_0^2}{\omega^2}}-\frac{1}{3}\right)-\left(1+\frac{1}{1-\frac{\omega_0^2}{\omega^2}}\right)\right] \quad (45)$$

The above formula (45) is valid only for $\omega > \omega_0$, because the waves with $\omega < \omega_0$ do not propagate in the plasma. One can see from (45) that when there is a vacuum, where $\omega_0 = 0$ and no deformation in spacetime where $\varepsilon = 0$ It is a gravitational deflection.

$$\hat{\alpha}_b = 2\left(\frac{r_g}{b}\right) \quad (46)$$

This is the Schwarzschild formula. In the presence of plasma and in the absence of space-time deformation, formula (45) becomes:

$$\hat{\alpha}_b = \frac{r_g}{b}\left(\frac{1}{1-\frac{\omega_0^2}{\omega^2}}+1\right) \quad (47)$$

As shown by [29], it can easily be seen that, in the absence of plasma, the deflection angle by non-Schwarzschild space-time will be:

$$\hat{\alpha}_b = -2\frac{r_g}{b}\left(\frac{1}{3}\left(\frac{GM}{c^2 b}\right)^2\epsilon - 1\right) \quad (48)$$

To highlight the importance of our research, we compare the second term on the right-hand side of Eq. (45) with the deformation parameter for $\hat{\alpha}_b$, and the first term, by order of magnitude. The ratio of these terms is equal to a certain value when $\omega_0 \ll \omega$.

$$-\frac{1}{3}\epsilon\left(\frac{GM}{c^2 b}\right)^2 \quad (49)$$

Now, let us examine how the deflection angle behaves in a weak field for a lens with homogeneous plasma, as described by a non-Schwarzschild metric (38). As can be seen from (Figure 8), the deflection angle decreases with increasing impact parameter b for all values of the deformation parameter ϵ, whether the lens is in a vacuum (Figure 8a), or surrounded by plasma (Figure 8 b).
It should be noted that deflection can be strongest for radio waves when the frequency of the electromagnetic wave slightly exceeds the plasma frequency [30], and for other wavelengths when the frequency of light is much greater than the electron frequency in the plasma, resulting in a Schwarzschild value of Eq. (46).

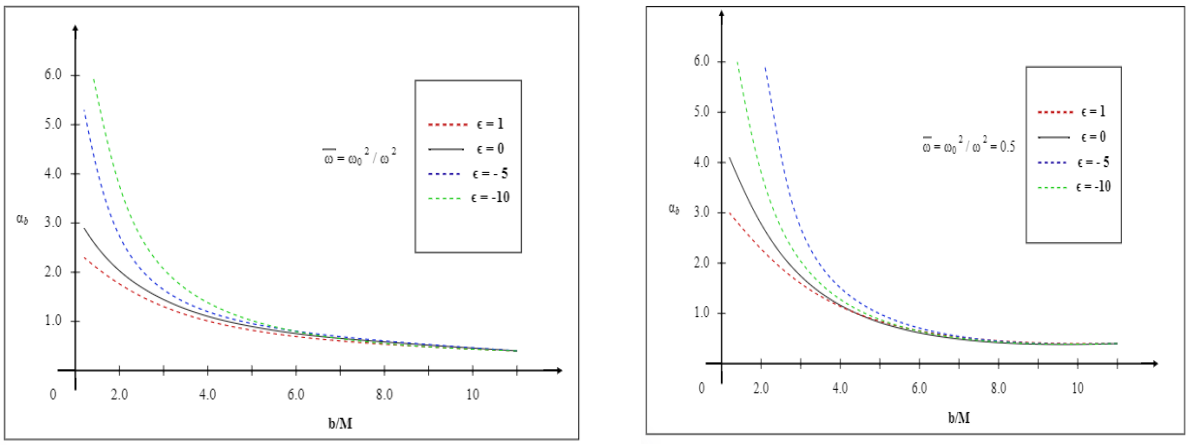

Figure 8. Deflection angle α_b as a function of the impact parameter

The change of deflection angle α by the deformed lensing object with a square ratio of electron frequency plasma ω_0 to the frequency of the photon ω changes from zero to one are shown in (Figure 9), which tells us that the deflection angle is increasing monotonically with frequency ω is approaching the electron plasma frequency ω_0.

Received: *21-06-2025* - ***Accepted***: *19-08-2025* - ***Published***: *26-08-2025*

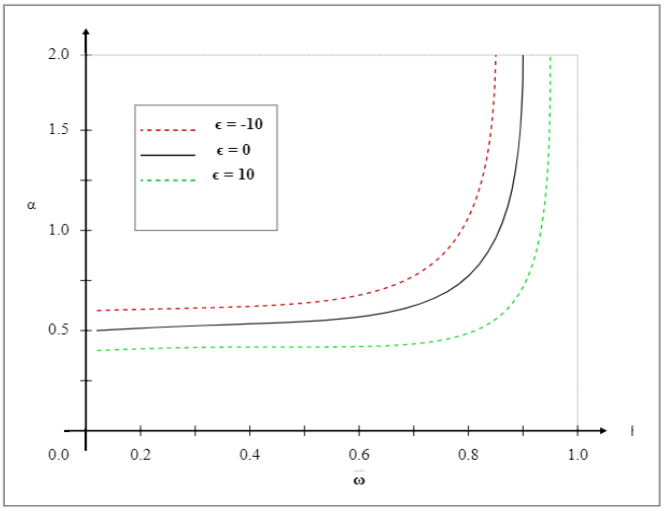

Figure 9. Illustrates the variety of the deflection angle α_b with the deformed parameter ϵ.

Conclusion

This study explores the influence of gravitational and plasma effects on light deflection and time delay in strong lensing systems. While gravitational deflection and refraction are typically negligible in simplified models, their combined impact becomes significant in the presence of plasma. Homogeneous plasma introduces chromatic gravitational deflection dependent on photon frequency, whereas non-homogeneous plasma contributes both chromatic gravitational and refractive deflection. These chromatic effects, observable primarily in long radio wavelengths, cause wavelength-dependent shifts in image positions and are detectable only in strong lens systems. The research also analytically examines time delays in plasma-rich environments, decomposing them into gravitational potential delay, geometric delay, and plasma-induced dispersion delay. Using the singular isothermal sphere model, plasma effects are incorporated as minor corrections to gravitational deflection—negligible in the optical range but notable in radio frequencies. Detectable discrepancies in image positions across spectral bands indicate the necessity of including plasma effects in lens modelling. Additionally, a literature review on gravitational lensing around deformed, non-Schwarzschild objects surrounded by plasma reveals that light deflection is proportional to both the gravitational mass and the deformation parameter (ε). The deformation-to-mass ratio observed may be comparable to that found in typical neutron stars.

Conflict of interest. Nil

References

1. Bisnovatyi-Kogan GS, Tsupko OY. Gravitational radiospectrometer. Gravitation and Cosmology. 2009;15:20-7.
2. Bisnovatyi-Kogan GS, Tsupko OY. Gravitational lensing in a non-uniform plasma. Mon Not R Astron Soc. 2010;404(3):1790-800.
3. Landau LD, Lifshitz EM. Electrodynamics of continuous media. Oxford: Pergamon Press; 1960.
4. Zhelezniakov VV. Electromagnetic waves in space plasma: generation and propagation. Moscow: Nauka; 1977. Russian.
5. Darwin C. The gravity field of a particle. Proc R Soc Lond A Math Phys Sci. 1959;249(1257):180-94.
6. Bisnovatyi-Kogan GS, Tsupko OY. Strong gravitational lensing by Schwarzschild black holes. Astrophysics. 2008;51(1):99-111.
7. Bozza V, Capozziello S, Iovane G, Scarpetta G. Strong field limit of black hole gravitational lensing. Gen Relativ Gravit. 2001;33(9):1535-48.
8. Congdon AB, Keeton C. Principles of gravitational lensing: light deflection as a probe of astrophysics and cosmology. Cham: Springer International Publishing; 2018.
9. Dodelson S. Gravitational lensing. Cambridge: Cambridge University Press; 2017.
10. Er X, Yang YP, Rogers A. Frequency-dependent effects of gravitational lensing in plasma. Astrophys J. 2020;889(2):158.
11. Wagner J, Er X. [Preprint]. 2020. arXiv:2006.16263.
12. Tsupko OY, Bisnovatyi-Kogan GS, Rogers A, Er X. Gravitational lensing in a non-uniform plasma: a broader view. Class Quantum Gravity. 2020;37(20):205017.
13. Hackmann E, Dhani A. Analytic gravitational waveforms and fluxes for particles on circular orbits in Kerr spacetime. Gen Relativ Gravit. 2019;51(3):37.
14. Schneider P, Ehlers J, Falco EE. Gravitational lenses. Berlin: Springer-Verlag; 1992.
15. Schneider P, Kochanek CS, Wambsganss J. Gravitational lensing: strong, weak and micro. Berlin: Springer; 2006. (Saas-Fee Advanced Courses; 33).
16. Congdon AB, Keeton C. Principles of gravitational lensing: light deflection as a probe of astrophysics and cosmology. Cham: Springer International Publishing; 2018.
17. Dodelson S. Gravitational lensing. Cambridge: Cambridge University Press; 2017.

Received: *21-06-2025* - ***Accepted***: *19-08-2025* - ***Published***: *26-08-2025*

18. Schneider P, Ehlers J, Falco EE. Gravitational lenses. Berlin: Springer-Verlag; 1992.
19. Schneider P, Kochanek CS, Wambsganss J. Gravitational lensing: strong, weak and micro. Berlin: Springer; 2006. (Saas-Fee Advanced Courses; 33).
20. Congdon AB, Keeton C. Principles of gravitational lensing: light deflection as a probe of astrophysics and cosmology. Cham: Springer International Publishing; 2018.
21. Bisnovatyi-Kogan GS, Tsupko OY. Gravitational radiospectrometer. Gravitation and Cosmology. 2009;15:20-7.
22. Bisnovatyi-Kogan GS, Tsupko OY. Gravitational lensing in a non-uniform plasma. Mon Not R Astron Soc. 2010;404(3):1790-800.
23. Perlick V, Tsupko OY, Bisnovatyi-Kogan GS. Influence of a plasma on the shadow of a spherically symmetric black hole. Phys Rev D. 2015;92(10):104031.
24. Perlick V, Tsupko OY. Calculating black hole shadows: review of analytical studies. Phys Rev D. 2017;95(10):104003.
25. Tsupko OY, Bisnovatyi-Kogan GS. Gravitational lensing in plasma: relativistic images at homogeneous plasma. Phys Rev D. 2013;87(12):124009.
26. Virbhadra KS, Ellis GFR. Schwarzschild black hole lensing. Phys Rev D. 2000;62(8):084003.
27. Virbhadra KS. Relativistic images of Schwarzschild black hole lensing. Phys Rev D. 2009;79(8):083004.
28. Landau LD, Lifshitz EM. The classical theory of fields. Elmsford (NY): Pergamon Press; 1971.
29. Bisnovatyi-Kogan GS, Tsupko OY. Gravitational lensing in a non-uniform plasma. Mon Not R Astron Soc. 2010;404(3):1790-800.
30. Bisnovatyi-Kogan GS, Tsupko OY. Gravitational radiospectrometer. Gravitation and Cosmology. 2009;15:20-7.

Received*: 21-06-2025 -* ***Accepted****: 19-08-2025 -* ***Published****: 26-08-2025*